Density of States-Based DC I–V Model of Amorphous Gallium–Indium–Zinc-Oxide Thin-Film Transistors

Jun-Hyun Park, Sangwon Lee, Kichan Jeon, Sunil Kim, Sangwook Kim, Jaechul Park, Ihun Song, Chang Jung Kim, Youngsoo Park, Dong Myong Kim, *Member, IEEE*, and Dae Hwan Kim, *Member, IEEE*

***Abstract*—The density of states (DOS)-based DC I–V model of an amorphous gallium–indium–zinc oxide (a-GIZO) thin-film transistor (TFT) is proposed and demonstrated with self-consistent methodologies for extracting parameters. By combining the optical charge-pumping technique and the nonlinear relation between the surface potential (ϕ_S) and gate voltage ($V_{\rm GS}$), it is verified that the proposed DC model reproduces well both the measured $V_{\rm GS}$-dependent mobility and the $I_{\rm DS}$–$V_{\rm GS}$ characteristics. Finally, the extracted DOS parameters are $N_{\rm TA} = 4.4\times10^{17}$ cm$^{-3}\cdot$eV^{-1}, $N_{\rm DA} = 3\times10^{15}$ cm$^{-3}\cdot$eV^{-1}, $kT_{\rm TA} = 0.023$ eV, $kT_{\rm DGA} = 1.5$ eV, and $E_O = 1.8$ eV, with the formulas of exponential tail states and Gaussian deep states.**

***Index Terms*—Amorphous, DC model, density of states (DOS), GaInZnO, thin-film transistors (TFTs).**

I. Introduction

VERY recently, amorphous gallium–indium–zinc oxide (a-GIZO) thin-film transistors (TFTs) have emerged as promising building blocks in applications such as flat-panel-display backplanes [1]–[3], electronic papers, and peripheral circuits in 3-D stacked memories [4]. However, the theoretical approach with physical parameters (not fitting parameters) determining the bias dependences of carrier density n, channel mobility μ, and on-current $I_{\rm DS}$ has been rarely reported, although it is essential to the device model for circuit simulation. Recognizing that the device model reflecting the physical mechanism is indispensable for the design of various innovative application-oriented circuits, the importance of the DC model of a-GIZO TFTs with appropriate techniques for extracting concrete model parameters cannot be overemphasized. Motivated by these backgrounds, in our previous work, the density of states [DOS: $g(E)$ (per cubic centimeter per electron volt)] of a-GIZO active layer has been experimentally extracted by combining the optical charge-pumping and C–V characteristics [5]. However, the presumption of a linear relation between the surface potential (ϕ_S) and gate voltage ($V_{\rm GS}$) should be overcome for a more accurate DC/AC model under wider bias range.

In this letter, the nonlinear $\phi_S - V_{\rm GS}$ relation-based DC I–V model of an a-GIZO TFT is proposed and demonstrated by using a self-consistent parameter-extracting technique. The key parameters are the a-GIZO active layer $g(E)$, intrinsic channel mobility ($\mu_{\rm CH}$), and parasitic resistances (including source/drain (S/D) spreading/series and contact resistance components) (R_P). The proposed models are verified by comparison with the measured $\mu_{\rm CH}$ and I–V characteristics.

II. Device Structure

The fabricated TFT has an inverted staggered bottom gate, and the a-GIZO active layer is deposited by RF magnetron sputtering at room temperature. The detailed process sequences are the same with that in [5]. The gate-oxide thickness ($T_{\rm GI}$), a-GIZO active-layer thickness ($T_{\rm GIZO}$), channel length (L), channel width (W), and overlap length between the gate and S/D ($L_{\rm ov}$) are designed to be 100 nm, 70 nm, 50 μm, 200 μm, and 10 μm, respectively.

III. DOS-Based DC I–V Model

Fig. 1(a) shows the *preliminary DOS* of an a-GIZO active layer obtained by using the same method with that in [5]. The terminology of "preliminary DOS" means the DOS assuming the linear relation between ϕ_S and $V_{\rm GS}$. The *final DOS* should be acquired by fully taking the complicated nonlinear relation between ϕ_S (consequently, E) and $V_{\rm GS}$ into account.

The localized trapped charge density ($n_{\rm loc}$) and free carrier density ($n_{\rm free}$) are expressed as

$$n_{\rm loc}(x) = \int_{E_V}^{E_C} g(E)\times f(E)dE \quad [{\rm cm}^{-3}] \tag{1}$$

$$n_{\rm free}(x) = N_C \times \exp\left(\frac{q\left(\phi(x) - \phi_{\rm CH} - \phi_{\rm FO}\right)}{kT}\right) \quad [{\rm cm}^{-3}] \tag{2}$$

where E_V, E_C, $f(E)$, N_C, $\phi(x)$, $\phi_{\rm CH}$, and ϕ_{F0} are the valence-band maximum, the conduction-band minimum, the Fermi-Dirac distribution function, the conduction-band effective DOS, the electrostatic potential along a channel depth x-direction, the Fermi-potential lowering by drain bias ($V_{\rm DS}$), and the Fermi potential at a thermal equilibrium, respectively, as shown in

Manuscript received June 23, 2009. First published September 9, 2009; current version published September 29, 2009. This work was supported by the Korea Science and Engineering Foundation (KOSEF) grant funded by the Korea government (MEST) (No. 2009-0080344). The CAD software was supported by SILVACO and IC Design Education Center (IDEC). The review of this letter was arranged by Editor J. K. O. Sin.

The authors are with the School of Electrical Engineering, Kookmin University, Seoul 136-702, Korea (e-mail: jhpark@kookmin.ac.kr; drlife@kookmin.ac.kr).

Color versions of one or more of the figures in this letter are available online at http://ieeexplore.ieee.org.

Digital Object Identifier 10.1109/LED.2009.2028042

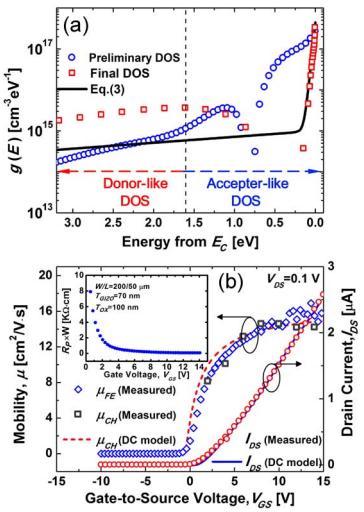

Fig. 1. (a) Various extracted DOSs of an a-GIZO TFT. The preliminary $g(E)$ is measured by combining the optical charge-pumping and C–V characteristics [5]. The final $g(E)$ is acquired by solving the DOS parameters through numerical iterations until satisfying two self-consistencies: the consistency between (3) and the nonlinearly mapped version of the preliminary $g(E)$, and that between (12) and the measured $I_{\rm DS}$–$V_{\rm GS}$ characteristics. Here, nonlinear mapping is performed by using (5) and (6). It is noticeable that only the lateral location of data points in the preliminary $g(E)$ is changed, even after reflecting the nonlinear relation between ϕ_S and $V_{\rm GS}$. Equation (3) corresponds to the DC model $g(E)$. The tail states of the final $g(E)$ agree well with those of the DC model $g(E)$. (b) $V_{\rm GS}$-dependent mobility and $I_{\rm DS}$–$V_{\rm GS}$ characteristics. The measured field-effect mobility ($\mu_{\rm FE}$) and intrinsic mobility ($\mu_{\rm CH}$) are consistent with the DC model $\mu_{\rm CH}$ calculated by using (10). In addition, the measured $I_{\rm DS}$–$V_{\rm GS}$ curve agrees well with the one calculated by using (12). The inset shows the $V_{\rm GS}$-dependent R_P extracted from the TLM method.

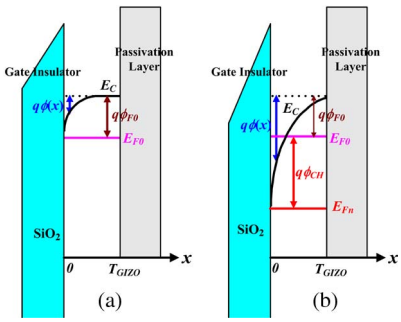

Fig. 2. Energy-band diagram of an a-GIZO TFT with definitions of $\phi(x)$, $\phi_{\rm CH}$, and ϕ_{F0} at the (a) source and (b) drain edge regions.

Fig. 2. If the DOS used in the DC model (*DC model DOS*) is given by

$$g(E) = N_{\rm TA} \times \exp\left(\frac{E-E_C}{kT_{\rm TA}}\right) + N_{\rm DA} \times \exp\left(\frac{E-E_C}{kT_{\rm DA}}\right) \quad [{\rm cm}^{-3}\cdot{\rm eV}^{-1}] \quad (3)$$

then $n_{\rm loc}$ can be calculated by using (1) and (3). Then, Poisson's equation along the x-direction from the interface between a-GIZO and gate oxide is redescribed as

$$\frac{\partial^2\phi(x)}{\partial x^2} = -\frac{\rho(x)}{\varepsilon_{\rm GIZO}} = \frac{q}{\varepsilon_{\rm GIZO}}\left(n_{\rm free}(x)+n_{\rm loc}(x)\right) \quad (4)$$

where $\varepsilon_{\rm GIZO}$ and ρ are the permittivity of the a-GIZO material and the volume charge density, respectively. Using the relationship of $2\times(\partial\phi(x)/\partial x)(\partial^2\phi(x)/\partial x^2) = \partial/\partial x(\partial\phi(x)/\partial x)^2$, the electric field $E_{\rm GIZO}$ at a specific x can be given as a function of the same DOS parameters as that in [6]

$$E_{\rm GIZO} = \sqrt{2\int_{\phi(x=T_{\rm GIZO})}^{\phi(x)} \frac{q}{\varepsilon_{\rm GIZO}}\left(n_{\rm loc}(x)+n_{\rm free}(x)\right)d\phi(x)}. \quad (5)$$

In order to obtain the nonlinear relation between $V_{\rm GS}$ and E, we apply the Gauss law to the interface of a-GIZO/gate oxide as follows:

$$V_{\rm GS} = V_{\rm FB}+\phi_S+\frac{Q_{\rm induced}}{C_{\rm ox}} = V_{\rm FB}+\phi_S+\frac{Q_{\rm free}+Q_{\rm loc}}{C_{\rm ox}} = V_{\rm FB}+\phi_S+\frac{\varepsilon_{\rm GIZO}E_{\rm GIZO}(\phi_S)}{C_{\rm ox}} \quad [{\rm V}] \quad (6)$$

where $Q_{\rm induced}$ is the $V_{\rm GS}$-dependent field-induced charge per unit area within the entire a-GIZO active layer and $V_{\rm FB}$ is the flatband voltage. By combining (5) and (6) with a numerical approach, the relation between $V_{\rm GS}$ and ϕ_S (eventually E) is derived as a function of DOS parameters.

On the other hand, as is the case of a-Si:H TFT, $\mu_{\rm CH}$ can be calculated as

$$\mu_{\rm CH}(\phi(x)) = \mu_{\rm BAND}\times\frac{Q_{\rm free}(\phi(x))}{Q_{\rm loc}(\phi(x))+Q_{\rm free}(\phi(x))} \quad \left[\frac{{\rm cm}^2}{{\rm V}\cdot{\rm s}}\right] \quad (7)$$

with $Q_{\rm free}$ and $Q_{\rm loc}$ are described as

$$Q_{\rm free}(\phi(x)) = q\int_x^{T_{\rm GIZO}} n_{\rm free}(\tau)d\tau \quad \left[\frac{\rm C}{{\rm cm}^2}\right] \quad (8)$$

$$Q_{\rm loc}(\phi(x)) = q\int_x^{T_{\rm GIZO}} n_{\rm loc}(\tau)d\tau = q\int_x^{T_{\rm GIZO}}\int_{E_V}^{E_C} g(E)\times f(E)dEd\tau \quad \left[\frac{\rm C}{{\rm cm}^2}\right]. \quad (9)$$

By taking into account (7) and changing the integration variable from x to $\phi(x)$ (with $E_{\rm GIZO} = -d\phi(x)/dx$), $\mu_{\rm CH}(x)$ becomes

$$\mu_{\rm CH}(x) = q\mu_{\rm BAND}\frac{\int_{\phi(x=T_{\rm GIZO})}^{\phi(x)}\frac{n_{\rm free}(\phi(x))}{E_{\rm GIZO}(\phi(x))}d\phi(x)}{\varepsilon_{\rm GIZO}\times E_{\rm GIZO}(\phi(x))} \quad \left[\frac{{\rm cm}^2}{{\rm V}\cdot{\rm s}}\right]. \quad (10)$$

Then, in order to derive the $I_{\rm DS}$–$V_{\rm GS}$ model, the drift conduction-current equation is introduced as

$$I_{\rm DS} = W\frac{dV_{\rm CH}}{dy}\int_{x=0}^{x=T_{\rm GIZO}} q\mu_{\rm CH}(x)\times n_{\rm free}(x)dx \quad [{\rm A}] \quad (11)$$

where $V_{\rm CH}$ and y are the channel potential and the position along the lateral (channel length) direction, respectively. By

substituting $\mu_{\rm CH}(x)$ in (10) for (11), we obtain $I_{\rm DS}$ as a function of $\phi(x)$.

By integrating $V_{\rm CH}$ from the source to the drain edge, one can calculate the $I_{\rm DS}$–$V_{\rm GS}$ model as follows:

$$I_{\rm DS} = W\frac{V'_{\rm DS}}{L}q\mu_{\rm BAND} \times \int_{\phi(x=T_{\rm GIZO})}^{\phi(x=0)} \frac{\int_{\phi(x=T_{\rm GIZO})}^{\phi(x)} \frac{qn_{\rm free}(\phi(x))}{E_{\rm GIZO}(\phi(x))}d\phi(x)}{\varepsilon_{\rm GIZO}\times E_{\rm GIZO}(\phi(x))} \times \frac{n_{\rm free}(\phi(x))}{E_{\rm GIZO}(\phi(x))}d\phi(x)$$

$$V'_{\rm DS} = V_{\rm DS} - (I_{\rm DS}\times R_P(V_{\rm GS})) \quad (12)$$

where $V'_{\rm DS}$ is the internal $V_{\rm DS}$. In order to take the R_P effect into account, $R_P(V_{\rm GS})$ was measured by using the same transmission-line modeling (TLM) method as that in [7] and [8], as shown in the inset of Fig. 1(b). It is noticeable in (12) that the $I_{\rm DS}$–$V_{\rm GS}$ model is expressed as a function of only ϕ_S [i.e., $\phi(x = T_{\rm GIZO})$] and/or $V_{\rm GS}$.

Thanks to (5) and (6), one can translate the *preliminary DOS* [seen in Fig. 1(a)] into the *final DOS*. However, in order to complete the translation of the *preliminary DOS* into the *final DOS* based on the nonlinear relation between E and $V_{\rm GS}$, the DOS parameters [$kT_{\rm TA}$, $kT_{\rm DA}$, $N_{\rm TA}$, and $N_{\rm DA}$ in (3)] should be known. Therefore, the *final DOS* was acquired by solving the DOS parameters through numerical iterations until satisfying two self-consistencies: the consistency between (3) and the nonlinearly mapped version of the measured *preliminary DOS*, and that between (12) and the measured $I_{\rm DS}$–$V_{\rm GS}$ characteristics. Here, it should be noted that only the lateral location of data points in the *preliminary DOS* is changed, even after reflecting the nonlinear relation between ϕ_S and $V_{\rm GS}$. Consequently, Fig. 1(a) shows both the *final DOS* and the *DC model DOS* [(3)], whose tail states are consistent with each other. It is found that the former has the formula

$$g(E) = N_{\rm TA}\times\exp\left(\frac{E-E_C}{kT_{\rm TA}}\right) + N_{\rm DA}\times\exp\left[-\left(\frac{E_O-E}{kT_{\rm DGA}}\right)^2\right]. \quad (13)$$

In the *final DOS*, the donorlike states should be further corrected due to the limitation of the optical charge-pumping technique [5]. In addition, the acceptorlike deep states of the *DC model DOS* (used in the calculation of the DC I–V model) are approximated into the exponential function for convenience, as shown in (3). Because the $V_{\rm GS}$-dependent trap filling above V_T is determined mainly from the tail states, our approximation is valid. The extracted DOS parameters are $N_{\rm TA} = 4.4\times10^{17}$ cm$^{-3}\cdot$eV^{-1}, $N_{\rm DA} = 3\times10^{15}$ cm$^{-3}\cdot$eV^{-1}, $kT_{\rm TA} = 0.023$ eV, $kT_{\rm DGA} = 1.5$ eV, and $E_O = 1.8$ eV for the *final DOS*, and $N_{\rm TA} = 4.4\times10^{17}$ cm$^{-3}\cdot$eV^{-1}, $N_{\rm DA} = 1\times10^{15}$ cm$^{-3}\cdot$eV^{-1}, $kT_{\rm TA} = 0.023$ eV, and $kT_{\rm DA} = 3$ eV for the *DC model DOS*.

As shown in Fig. 1(b), the measured $\mu_{\rm CH}$ and $I_{\rm DS}$–$V_{\rm GS}$ characteristics agree well with those calculated by using the *DC model DOS* parameters. The additional parameters were $N_{\rm C} = 4\times10^{18}$ cm^{-3}, $\mu_{\rm BAND} = 16.4$ cm^2/V$\cdot$s, $\varepsilon_{\rm GIZO} = 11.5\varepsilon_0$, and $V_{\rm FB} = -2.5$ V. Our results show the validity of the proposed DC I–V model, which is attributed to fully taking the nonlinear ϕ_S–$V_{\rm GS}$ relation into account with the experimentally extracted DOS.

IV. Conclusion

The nonlinear ϕ_S–$V_{\rm GS}$ relation-based DC I–V model of an a-GIZO TFT was proposed and demonstrated by using a self-consistent parameter-extracting technique. The key parameters were $g(E)$, $\mu_{\rm CH}$, and $\rm R_P$. The accuracy of the proposed models was proved by comparison with the measured $V_{\rm GS}$-dependent $\mu_{\rm CH}$ and $I_{\rm DS}$–$V_{\rm GS}$ characteristics. Because the proposed DC model makes it possible to calculate the $\mu_{\rm CH}$ and I–V characteristics from the measured process-dependent DOS parameters, our results are expected to play a significant role in the device design and modeling for the simulation of innovative application-oriented circuits based on a-GIZO TFTs such as wearable computers, paper displays, transparent displays, solar cells, and 3-D stacked memories.

References

[1] C. J. Kim, D. Kang, I. Song, J. Park, H. Lim, S. Kim, E. Lee, R. Chung, J. Lee, and Y. Park, "Highly stable Ga_2O_3–In_2O_3–ZnO TFT for active-matrix organic light-emitting diode display application," in *IEDM Tech. Dig.*, 2006, pp. 11.6.1–11.6.4.

[2] J. K. Jeong, J. H. Jeong, J. H. Choi, J. S. Im, S. H. Kim, H. W. Yang, K. N. Kang, K. S. Kim, T. K. Ahn, H.-J. Chung, and H. K. Chung, "12.1-inch WXGA AMOLED display driven by indium–gallium–zinc oxide TFTs array," in *Proc. Soc. Inform. Display Int. Symp. Dig. Tech. Papers*, 2008, pp. 1–4.

[3] J.-H. Lee, D.-H. Kim, D.-J. Yang, S.-Y. Hong, K.-S. Yoon, P.-S. Hong, C.-O. Jeong, H.-S. Park, S. Y. Kim, S. K. Lim, S. S. Kim, K.-S. Son, T.-S. Kim, J.-Y. Kwon, and S.-Y. Lee, "World's largest (15-inch) XGA AMLCD panel using IGZO oxide TFT," in *Proc. Soc. Inform. Display Int. Symp. Dig. Tech. Papers*, 2008, pp. 625–628.

[4] M.-J. Lee, C. B. Lee, S. Kim, H. Yin, J. Park, S. E. Ahn, B. S. Kang, K. H. Kim, G. Stefanovich, I. Song, S.-W. Kim, J. H. Lee, S. J. Chung, Y. H. Kim, C. S. Lee, J. B. Park, I. G. Baek, C. J. Kim, and Y. Park, "Stack friendly all-oxide 3D RRAM using GaInZnO peripheral TFT realized over glass substrates," in *IEDM Tech. Dig.*, 2008, pp. 85–88.

[5] J.-H. Park, K. Jeon, S. Lee, S. Kim, S. Kim, I. Song, C. J. Kim, J. Park, Y. Park, D. M. Kim, and D. H. Kim, "Extraction of density of states in amorphous GaInZnO thin film transistors by combining an optical charge pumping and capacitance–voltage characteristics," *IEEE Electron Device Lett.*, vol. 29, no. 12, pp. 1292–1295, Dec. 2008.

[6] S.-S. Chen and J. B. Kuo, "An analytical a-Si:H TFT DC/capacitance model using an effective temperature approach for deriving a switching time model for an inverter circuit considering deep and tail states," *IEEE Trans. Electron Devices*, vol. 41, no. 7, pp. 1169–1178, Jul. 1994.

[7] J. Zaumseil, K. W. Baldwin, and J. A. Rogers, "Contact resistance in organic transistors that use source and drain electrodes formed by soft contact lamination," *J. Appl. Phys.*, vol. 93, no. 10, pp. 6117–6124, May 2003.

[8] P. Barquinha, A. M. Vila, G. Gonçalves, L. Pereira, R. Martins, J. R. Morante, and E. Fortunato, "Gallium–indium–zinc-oxide-based thin-film transistors: Influence of the source/drain material," *IEEE Trans. Electron Devices*, vol. 55, no. 4, pp. 954–960, Apr. 2008.